

# We are IntechOpen, the world's leading publisher of Open Access books Built by scientists, for scientists

6,900

Open access books available

185,000

International authors and editors

200M

Downloads

Our authors are among the

154

Countries delivered to

TOP 1%

most cited scientists

12.2%

Contributors from top 500 universities



WEB OF SCIENCE™

Selection of our books indexed in the Book Citation Index  
in Web of Science™ Core Collection (BKCI)

Interested in publishing with us?  
Contact [book.department@intechopen.com](mailto:book.department@intechopen.com)

Numbers displayed above are based on latest data collected.  
For more information visit [www.intechopen.com](http://www.intechopen.com)



# A Defected Metasurface for Field-Localizing Wireless Power Transfer

*Sarawuth Chaimool, Chawalit Rakluea, Yan Zhao  
and Prayoot Akkaraekthalin*

## Abstract

The potential of wireless power transfer (WPT) has attracted considerable interest for various research and commercial applications for home and industry. Two important topics including transfer efficiency and electromotive force (EMF) leakage are concerned with modern WPT systems. This work presents the defected metasurface for localized WPT to prevent the transfer efficiency degraded by tuning the resonance of only one-unit cell at the certain metasurface (MTS). Localization cavities on the metasurface can be formed in a defected metasurface, thus fields can be confined to the region around a small receiver, which enhances the transfer efficiency and reduces leakage of electromagnetic fields. To create a cavity in MTS, a defected unit cell at the receiving coils' positions for enhancing the efficiency will be designed, aiming to confine the magnetic field. Results show that the peak efficiency of 1.9% for the case of the free space is improved to 60% when the proposed defected metasurface is applied, which corresponds to 31.2 times enhancements. Therefore, the defected MTS can control the wave propagation in two-dimensional of WPT system.

**Keywords:** localization, wireless power transfer, metasurface, magneto inductive wave, reduced EMF

## 1. Introduction

Nowadays, wireless technologies are important on our life societies. It is not only on emerging wireless communication systems e.g., 5G, WiFi6, but also on wireless power transfer (WPT) systems. A WPT system can deliver the electrical energy from one to another across the air gap without the need for wires or exposed contacts. An example of the most commonly used WPT is the charging systems of mobile phones and electronics gadget devices. Recently, iPhone12 has been released and all models feature wireless charging [1]. Its power is up to 15 W with the most up-to-date Qi- standard [2]. However, most of the mobile wireless charging is not truly wireless because a phone needs to touch a charging station. Another application of WPT technology is an electric vehicle (EV) charging station [3–5], which requires high power and without touching the charging station. The required power is up to a few kilowatts. Although the two systems seem different, both share the same technique, which are used in a near-field WPT. The near-field WPT can be

categorized into two types: inductive coupling and magnetic resonance coupling [6]. Usually, the inductive coupling technique is lowering efficiency and shorter distance compared to the magnetic resonance method. The magnetic resonance method is based on the resonant coupling with two-same frequency resonant circuits while it is interacting weakly with other off-resonant frequency. Therefore, many studies have been proposed the techniques to improve efficiency and operating distance [7–10]. Moreover, a near-field WPT system is using magnetic field coupling and uses in high power applications, so electromagnetic fields (EMFs) accordingly increase. Hence, leakage EMF emitted from WPT system should follow the feasible guideline of ICNIRP (International Commission on Non-Ionizing Radiation Protection (ICNIRP) [11]. It can be damaging human bodies and surroundings. To meet safety requirements below a certain standard level, most of the previous works have been proposed using ferrite and metallic shields [12–14]. The ferrite-based shielding is moderately effective, but it is very heavy weight and normally used in low-frequency. While the metallic-based shielding is flatter and more lightweight, the reflected wave can degrade the overall efficiency of the WPT system. Both transfer efficiency and EMF leakage are concerned in modern WPT. Unfortunately, each proposed technique can solve only one by one. Recently, the use of electromagnetic metamaterials (MTM)/metasurface (MTS) for WPT systems have been proposed [15–19]. Metamaterials are engineered composites that exhibit unusual electromagnetics properties, which are not found in natural materials. Usually, implemented MTMs/MTSs are always used a uniform, which all unit cell is identical. Unfortunately, the most property of the uniform MTM/MTS is negative permeability, which can enhance only the transfer efficiency with evanescent wave amplification, hence increasing transfer efficiency. Consequently, many research efforts have been improved the transfer efficiency and decreased leakage electromagnetic fields (EMF) simultaneously. Recently, MTM/MTS have been proposed for enhancing the transfer efficiency and decreasing EMF leakage [20–25]. To solve both efficiency and safety problems, the non-uniform [18] and hybrid MTM/MTS techniques [22] have been proposed, however, these are suitable for the size of transmitting and receiving coils are comparable. Another method is using magneto-inductive wave (MIW), which is supported by MTM/MTS composed of inductively coupled electrically small resonators and created by inter-element couplings [26–29]. The MIWs can be constructed in one, two and three dimensions. Usually, however, the efficiency is fluctuation due to the standing MIW, which depends on the receiver position [27]. Moreover, the two-dimension MIWs have more complex dispersion [27, 29].

In practical various applications, a receiving side such as charging portable or implantable devices is usually smaller than a transmitting side. Moreover, users prefer to be able to freely location the receiving devices. When the receiver size is reduced to the transmitter, the efficiency rapidly decreases either with or without the MTM/MTS. This is because power distribution is spread out and unrefined above the charging surface; that is the transfer efficiency is variation when a receiving device position is misaligned, which is deviated from the concentric position with respect to a transmitter [19]. To refine and control the magnetic field by focusing the fields into the small regions, the non-uniform and defected MTSs with modified field localization technique have been proposed [20, 25, 30, 31]. The defected MTS is formed by the cavities on MTS. To create a cavity, a defected unit cell at the small receiving coils' positions can be designed and controlled by tuning the resonant frequency using external capacitor. The defected unit cell can be locally modified for magnetic field control at subwavelength scale. In addition, it does not change the macroscopic parameters including negative permeability. Unlike the previous approach [20, 25, 30], the receiver location is placed at center of

the MTS. There are different mechanisms to create the cavity on the MTS. In [30], the cavity is created by Fano-type interference, while the hybridization bandgap is used in [20] and MIW is applied in [25]. Motivated by these observations, we modify the cavity mode concept to create a new defected metasurface (MTS) for enhancing transferred efficiency and reducing the electromotive force (EMF). The MTS is based on a defected unit cell at the desired receiving position formed a two-dimensional cavity with configuration of the conventional WPT system. Besides, a free space case, a conventional uniform MTS and the proposed defected MTS have been studied and compared.

## 2. System configuration and metasurface characteristics

### 2.1 System configuration

A common WPT system consists of a transmitting coil and a receiving coil. Firstly, we investigate four configurations of the conventional WPT systems with and without uniform metasurface: (i) large Tx and large Rx coils (LTLR) without metasurface, (ii) large Tx coil and small Rx coil (LTSR) without metasurface, (iii) LTLR with uniform metasurface, and (iv) LTSR with uniform metasurface as shown in **Figure 1(a)** to **Figure 1(d)**, respectively. These four configurations are the reference configurations to compare with the proposed defected metasurface. The large size of coils is compared with the unit cell size of an MTS. For uniform MTS, all unit cells are identical, and its property is the negative effective permeability. The transmitting and receiving coils are used planar four-coils WPT system configuration and the operating frequency is 13.56 MHz band, which is an ISM (Industrial, Scientific and Medical) band. The large transmitting coil composes of the feed/load coil and three-turns planar resonator coil with a trace width of 3 mm and 17 mm. The gap between the adjacent loop of the resonator coil is 5 mm with the largest diameter of 240 mm. The radius of the feed/load coil is 48.5 mm. Due to the requirement of ISM bands; it is vital to fix the resonant frequency of WPT system. To resonate at a desired frequency of 13.56 MHz, a 68 pF chip capacitor is connected in series. The details are shown in **Figure 1(a)**. For the purposes of comparison, two different sizes of the receiving coil are examined. The first size of the receiving coil is identical to the large transmitting coil and the second one is smaller than the transmitting coil about five times, which the largest diameter is 60 mm. It is a two-turn planar coil and loaded with two capacitors at the driving loop coil and resonant loop coil. The detailed design of the two-turn planar coil is similar to our proposed in [32]. To enhance the efficiency and focus the magnetic

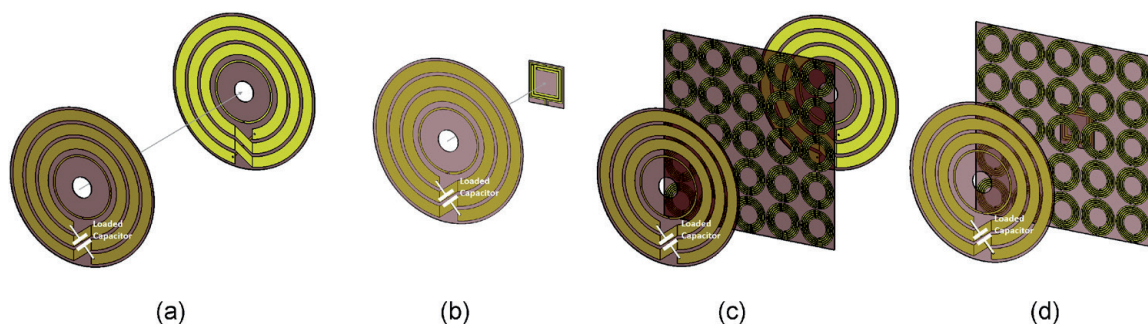


**Figure 1.** Configuration of the conventional WPT system. (a) large Tx and large Rx coils (LTLR) without metasurface, (b) large Tx coil and small Rx coil (LTSR) without metasurface, (c) LTLR with uniform metasurface, and (d) LTSR with uniform metasurface.

field, the uniform MTS is placed between the transmitting and receiving coils as shown in **Figure 1(c)** and **Figure 1(d)**. All transmitting coil, receiving coil and unit cell are designed on FR-4 material with a dielectric constant ( $\epsilon_r$ ) of 4.3 and loss tangent ( $\tan \delta$ ) of 0.025.

Then, to study the performance of the proposed defected metasurface on the WPT system, a system configuration is shown in **Figure 2**. It is composed of three parts including a transmitting coil, a defected MTS and a receiving coil. For the LTLR cases, the separation between the transmitting-to-metasurface and receiving-to-metasurface is the equal to 240 mm, so the distance from the transmitting to receiving coils is the total 480 mm as shown in **Figure 2(a)**. As we mentioned previous section, users prefer to able to freely location the receiver. A model of freely multiple receiver locations shows in **Figure 2(b)**. This configuration is not only freely movement the receiver, but also like misalignment between transmitter and receiver when the location is positioned on No. 2 to No. 6, so the efficiency deviates from the center (No. 1). Then, the effects of localization field have been extensively studied when the small receiving coil is placed closer to the defected MTS as shown in **Figure 2(b)**. The distance between the small receiving coil and the defected MTS is 40 mm, whereas the transmitting side is keeping the same. Numbers (No. 1 to No. 6) on unit cells are positioned of the cavities or hotspots formed in the defected MTS. The defected unit cell formed cavity is designed with different resonant frequencies from the uniform MTS. The resonant frequency of the defected unit cell is higher than the uniform one, which can be tuned by using the series chip capacitors. We examine the effects of the positions on the defected MTS using an EM simulator and measurement. The results will show and discuss in the following sections.

## 2.2 Metasurface characteristics

The metasurface is usually constructed using locally resonant unit cells in the deep subwavelength scale. For realized a compact metasurface and compromise between magnetic field enhancement, an array of  $5 \times 5$ -unit cells is chosen in this work. Each unit cell is a single-side planar 5-turn spiral with loaded a capacitor in order to resonate at the desired frequency as shown in **Figure 3(a)**. A loading capacitor of 117 pF is used to resonate at 11.88 MHz. It can be seen in **Figure 3(a)**

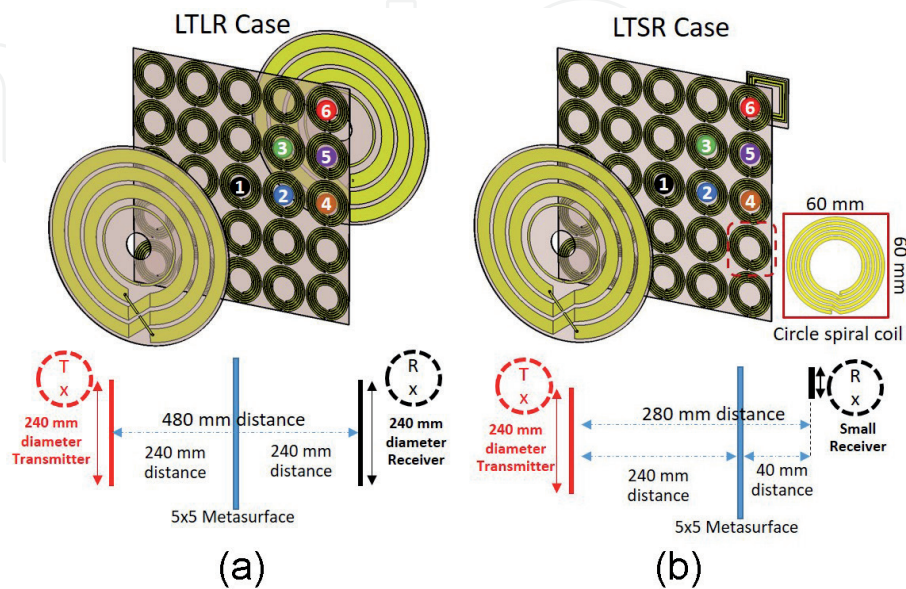


**Figure 2.** Configuration of the proposed defected metasurface. (a) LTLR and (b) LTSR. The defected positions are numbering from No. 1 (center) to No. 6.

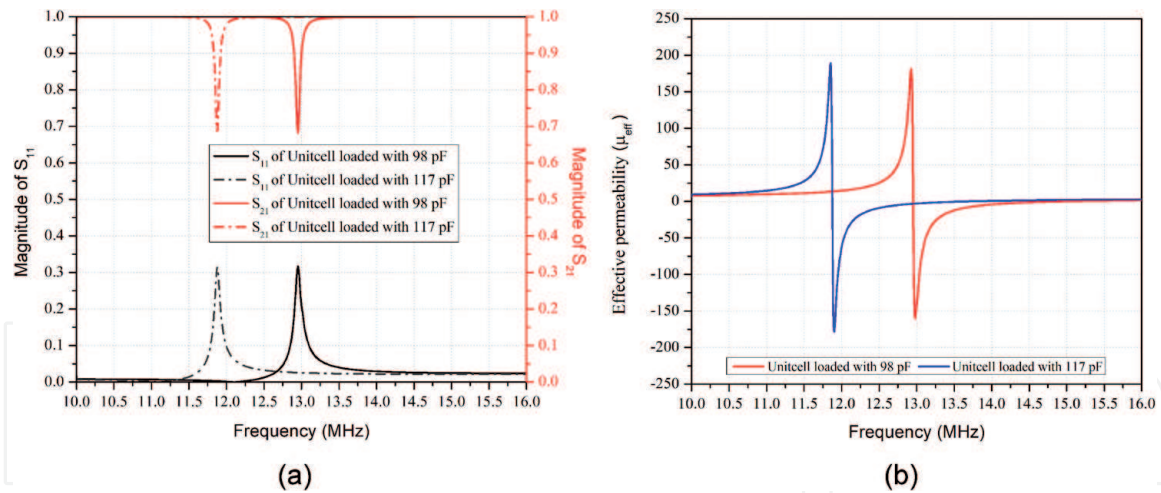


**Figure 3.** Metasurface characteristics (a) resonant frequency and (b) effective permeability.

that the resonant frequencies of 117 pF and 98 pF loadings are 11.88 MHz and 12.95 MHz, respectively. The frequency response of the 98 pF loading is also shown and compared because this configuration is designed for the selective created cavity. The resonant frequency of the cavity is slightly higher than the uniform unit cell. Then, the effective permeability of the proposed MTS can be obtained by using the CST simulation [33] with extracting the S-parameters of the proposed unit-cell as shown in **Figure 3(b)**. Since the WPT system is based on magnetic field coupling when an incident EM wave with a magnetic field is perpendicular to the plane of the MTS, the MTS obeys the frequency dispersive Lorentz model to produce an effective negative permeability. At 13.56 MHz, the effective permeability of both capacitor-loading achieves the negative permeability. To adjust the resonant frequency, it can be changed to the series capacitor [18].

### 3. Results and discussion

To compare the transfer efficiency ( $\eta$ ) of all configurations, we use the magnitude of  $|S_{21}|$ , which can be easily measured using a vector network analyzer (VNA) in experiments. By using the  $|S_{21}|$  and  $|S_{11}|$ , the function of the transfer efficiency on  $\eta = |S_{21}|^2 / (1 - |S_{11}|^2)$ , however, when the network is matching at both ports, the transfer efficiency equals  $|S_{21}|^2$ . A comparison of simulated  $|S_{21}|$  for the four reference cases and the LTLR with the defected MTS (**Figure 2(a)**) is shown in **Figure 4**. Compared with the free space, the magnitude of  $S_{21}$  is increased when a uniform or a defected MTS is used. At 13.56 MHz, the uniform MTS case has a maximum power transfer. It can be observed that a case of free-space case (without MTS) and the uniform MTS have only a single peak. The magnitude of  $S_{21}$  for the free-space case ( $|S_{21}| = 0.24$ ) is remarkable to lower compared with the case of the uniform MTS ( $|S_{21}| = 0.69$ ). When the defected unit cell is placed in each position, the magnitudes of  $|S_{21}|$  are separated into two or more peaks, called *frequency splitting*, which its mechanism is totally different from the two-coil system as a function of separation distance between coils. In a two-coil system, generally, when the distance between transmitting and receiving coils is closer and smaller than a threshold value, it creates two frequency splitting due to the magnetic over-couplings. Hence, many research efforts have been developed the system performance against frequency splitting using optimizing and compensation methods such as non-identical resonant coil [34]. The frequency splitting phenomenon of the defected MTS occurs when non-identical resonant unit cells. It can be explained in terms of Fano

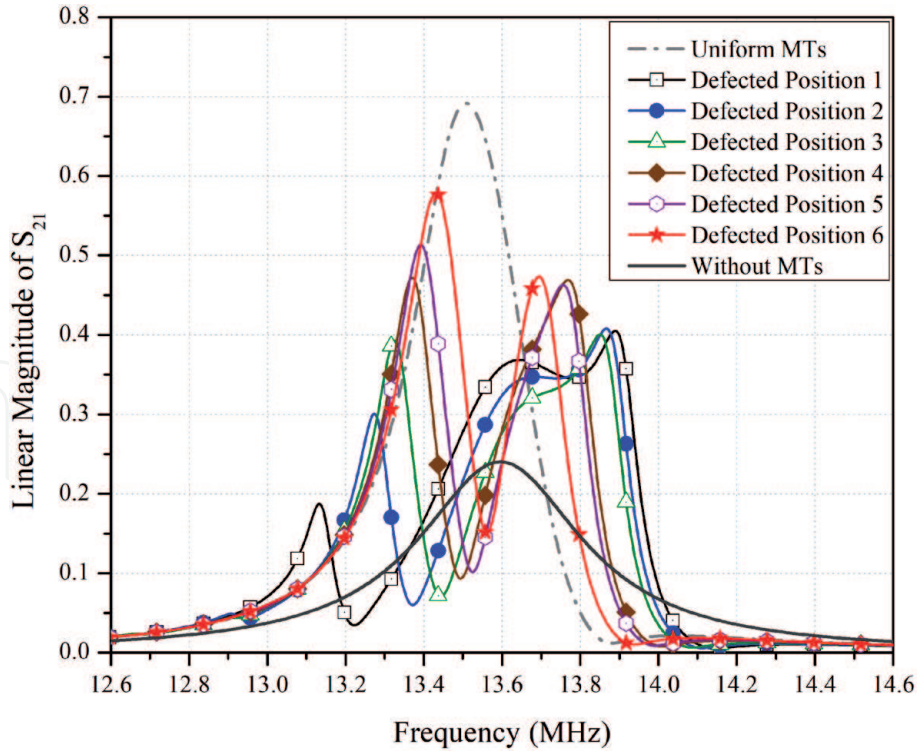


**Figure 4.**  
Comparison of simulated  $|S_{21}|$  for LTLR depending on the frequency.

interference [30, 35], which is much more sensitive to the defected position in its periodicity. It is observed that there are two peaks and the first one is smaller than the second one except two positions of No. 5 and No. 6. The first peak of the separating frequency is shifted to close the resonant frequency (13.56 MHz) when the defected position moves away from the center. As the defected position moves outward to the center of the MTS, the  $|S_{21}|$  and the frequency of the first peak also slowly increased accordingly. At the defected position of No. 4, the magnitude of  $|S_{21}|$  gets the minimum of 0.106 at 13.56 MHz. From the results, thus, the defected MTS for the cases of the large transmitting and receiving coils has not improved the efficiency due to the magnetic field confinement on the defected cell, as shown in **Figure 5(c)**.

In practice, a transmitting side with a larger coil size than a receiving side for charging portable and implantable devices is used. The typical relative size ratio between transmitting and receiving coils is large, so the efficiency results low. The configurations for a large transmitting side and a small receiving side with uniform and defected MTSs are shown in **Figure 1(d)** and **Figure 2(b)**, respectively. A comparison of the  $|S_{21}|$  at six positions for uniform and defected MTSs is shown in **Figure 6**. It can be seen in **Figure 6(a)** for uniform MTS that the  $|S_{21}|$  has a significant deterioration when the receiving coil move outward from the center. The difference  $|S_{21}|$  at 13.56 MHz between position No. 1 (center) and No. 6 is about 0.42 or 10 dB down, when the maximum is 0.61 at the receiving position in the center. **Figure 6(c)** shows the  $|S_{21}|$  of both uniform and defected MTSs at each receiving position. For the uniform MTS, the magnitude gradually decreases from 0.61 to 0.19 when the receiving coil moves from the center (No. 1) to the edge (No. 6) of the MTS.

Meanwhile, the defected MTS shows a  $|S_{21}|$  from 0.64 to 0.57. This is confirmed that the proposed defected MTS provides a relatively constant transfer efficiency in all the areas of the MTS. In addition, the defected MTS provides increased transfer efficiency compared with the cases of the free space and uniform one. This proposed configuration is in contrast of the [20, 24], which is constructed in the

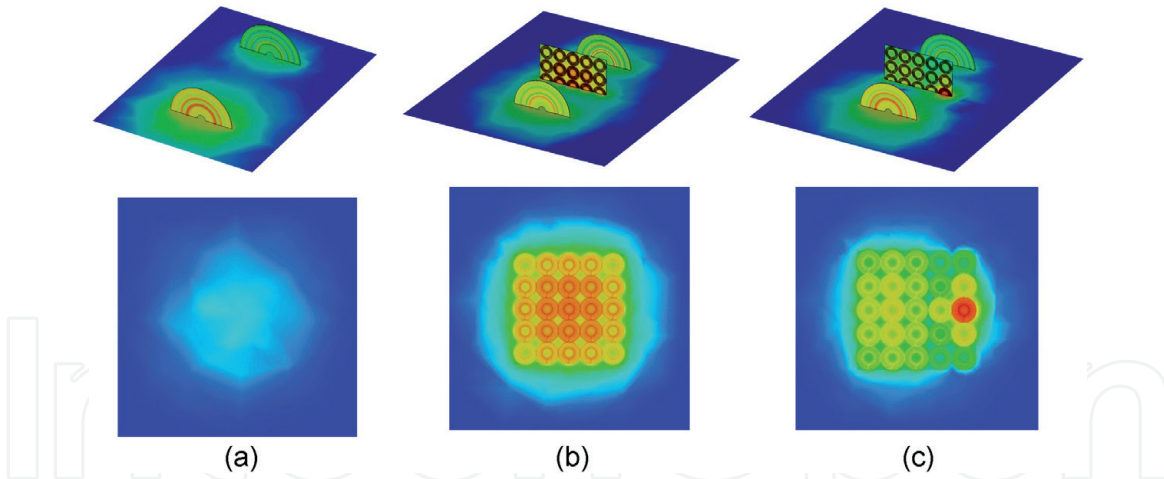


**Figure 5.** Magnetic field intensity distribution for LTLR (a) free space, (b) uniform MTS when the receiver at the center and (c) defected MTS when the receiver located at No. 4.

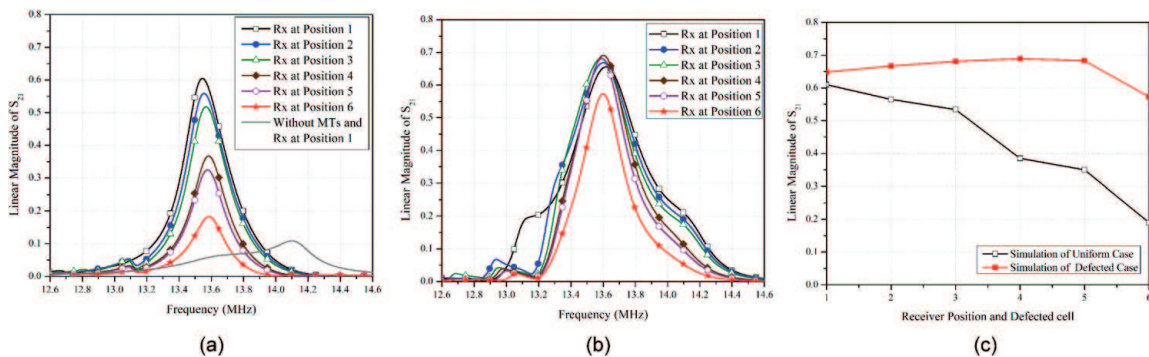


**Figure 6.** Comparison of the  $|S_{21}|$  for LTLR with different positions of the receiving coil on (a) the uniform MTS, (b) the defected MTS when the defected unit cell is the same position with the receiving coil and (c) both uniform and defected MTSs.

cavity using an array of the defected unit cells. So, the proposed defected MTS can enhance the transfer efficiency, even with its own loss.

The magnitudes of the magnetic field distribution are also used to compare between the WPT systems as shown in **Figure 5**. When whether the uniform or defected MTSs are inserted in the system, strong surface waves existing on both sides of the MTS are observed, which are responsible for the increased magnetic coupling. Obviously, the magnetic field intensity of free space is relatively weak in comparison with the metasurface cases. In case of free-space and the uniform MTS with the LTLR, the receiving coil is placed at the center. The intensity for both cases at the center is more concentrated than at the edge and the uniform MTS has a higher since the magnetic field is enhanced and focused by the negative permeability of the uniform MTS. In the case of the uniform MTS in **Figure 5(b)**, it is showed that the focusing effect of the magnetic field is present due to the negative refractive lens, which the field gradually decays from the center to the edge so, lead to better efficiencies. When the defected unit cell is selected at No. 4 as shown in **Figure 5(c)**, the focusing effect of the magnetic field is presented at position No. 4. However, For the other unit cell of the defected metasurface, the magnetic field intensity is significantly dropped compared with the case of the uniform MTS. According to the magnetic field distribution, the magnitude  $S_{21}$  value of the case of the defected metasurface is not too high, as the case of the uniform metasurface at a frequency of 13.56 MHz, as shown in **Figure 4** because the magnetic field intensity is confined only specific position.

**Figure 7** shows the magnetic field intensity distributions of LTSR with the uniform and defected MTSs at 13.56 MHz, respectively. On the uniform MTS in **Figure 7(a)**, the magnetic field spreads over a relative area, while the defected MTS shows that the focusing effect of the magnetic field from the cavity is presented, which can suppress the field elsewhere. It is observed in **Figure 7(b)** that the strong magnetic field confinement is realized on the defected MTS at the receiving position and the field is relatively low with uniform outside the cavity. It means that the defected MTS creates the field localization, hence, it can enhance transfer efficiency for a small receiver and reduce leakage EMF. It is because the unit cell forming the cavity resonance while the surrounding cells resonance at lower frequency. When the resonant frequency of surrounding cells falls into the hybridization bandgap, the negative permeability of metasurface forms a stopband for the cavity. Thus, the magnetic fields are prohibited from propagation in an outside area than the cavity. For the uniform MTS, the magnitude of the magnetic field is distributed relatively evenly about 14–22 dB along the surface of the MTS whereas the defected MTS is below 6 dB. Therefore, the defected MTS can enhance not only the field at the receiving coil, but also suppress the field elsewhere without additional shielding box or ferrite.

To experimentally validate the performance of the uniform and defected MTSs, several experimental studies are conducted. **Figure 8** shows the prototype of the proposed metasurface and experimental setup by using the VNA (Rohde & Schwarz model ZVB20). The fabricated MTS consists of  $5 \times 5$  arrays of unit cells that are

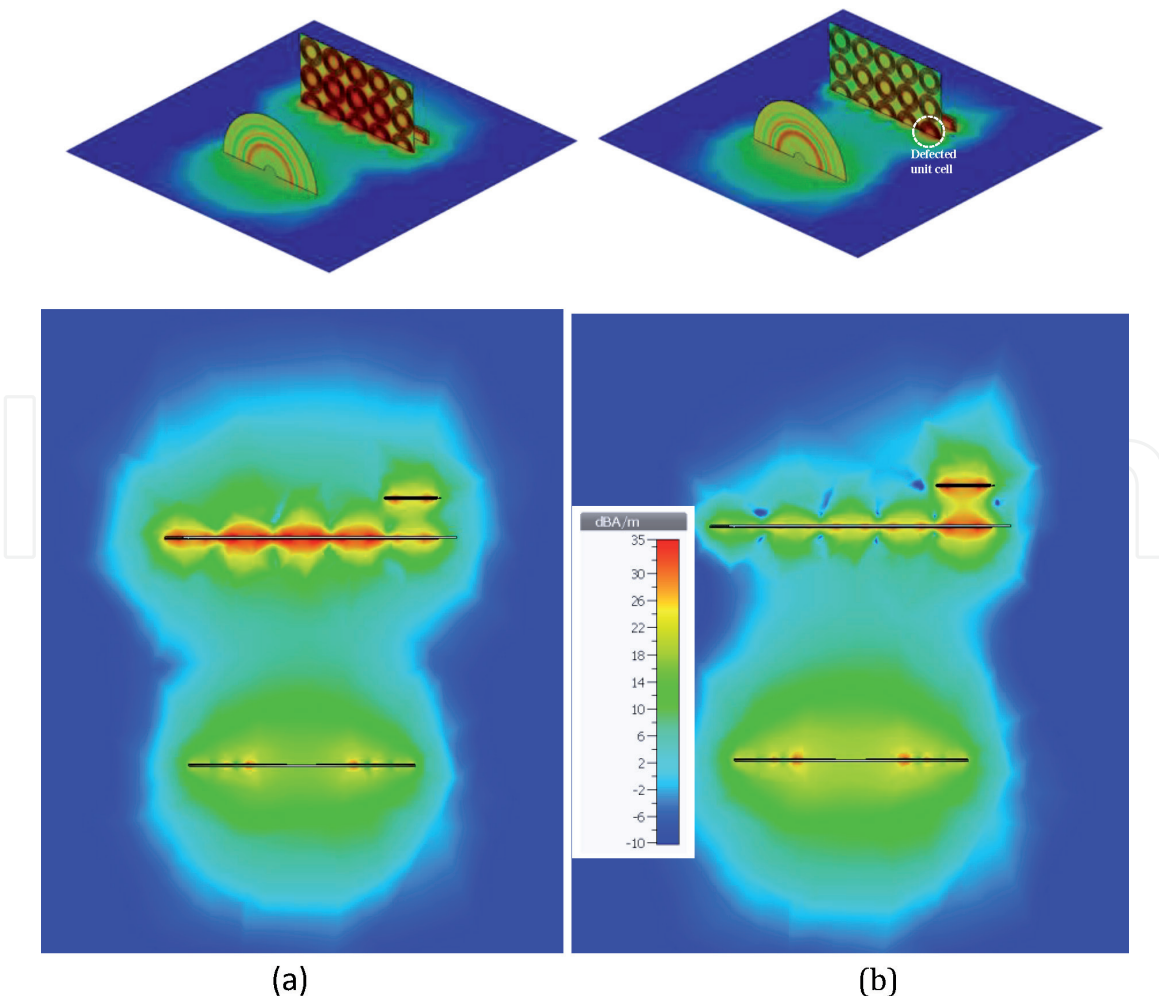


**Figure 7.** Magnetic field intensity distribution for LTSR when the receiver located at No. 4 (a) uniform MTS and (b) defected MTS.

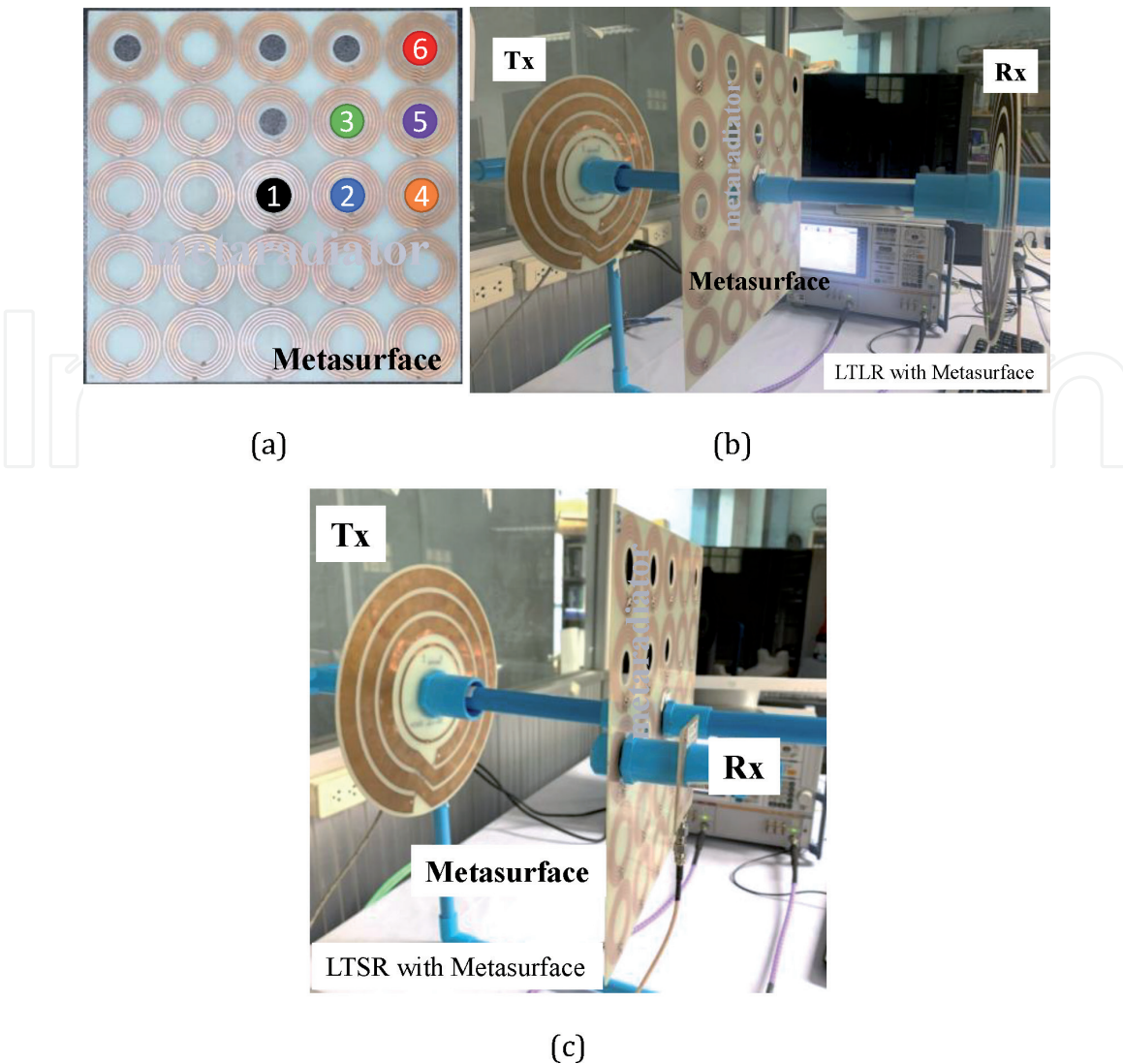


**Figure 8.** Photograph of prototype of the proposed metasurface (a) and the system experimental setup for measurement: (b) LTLR and (c) LTSR.

controlled individually using a chip capacitor as shown in **Figure 8(a)**. **Figure 8(b)** depicts the LTLR with the metasurfaces. In case of LTLR (**Figure 8(b)**), the large receiving is not fixed at the center, but it is moved and located following the defected unit cell. **Figure 8(c)** shows the case of the LTSR with the metasurfaces when the receiving coil can move all the unit cell locations. The distance between the receiving coil and MTS is fixed and kept by using the plastic pipe. It is a thin and non-magnetic material; its effect is negligible. The connection is accomplished using standard SMAs through two identical low-loss cables. The standard SOLT (short-open-line-trough) calibration has been performed at the desired frequency range before measurement, so the end of the cables has been considered as a reference plane for S-parameters. **Figure 9** shows the measured results of LTLR and LTSR cases with the uniform and defected MTSs, respectively. **Figure 9(a)** shows variation of the measured efficiency depending on the defected positions and the defected cell at position No. 0 is a uniform MTS case. As seen, the efficiency shows a significant dependence on the receiving positions. The WPT system is directly measured at the operating frequency of 13.56 MHz and using two-port method with VNA. It is clearly seen in **Figure 9(b)** that the transfer efficiency of the defected MTS is quite flat; it means the defected MTS can enhance the efficiency regardless of the positions of the receiving coil with various distances. **Figure 9(b)** shows the simulated and measured power transfer efficiency of LTLR and LTSR cases with the uniform and defected

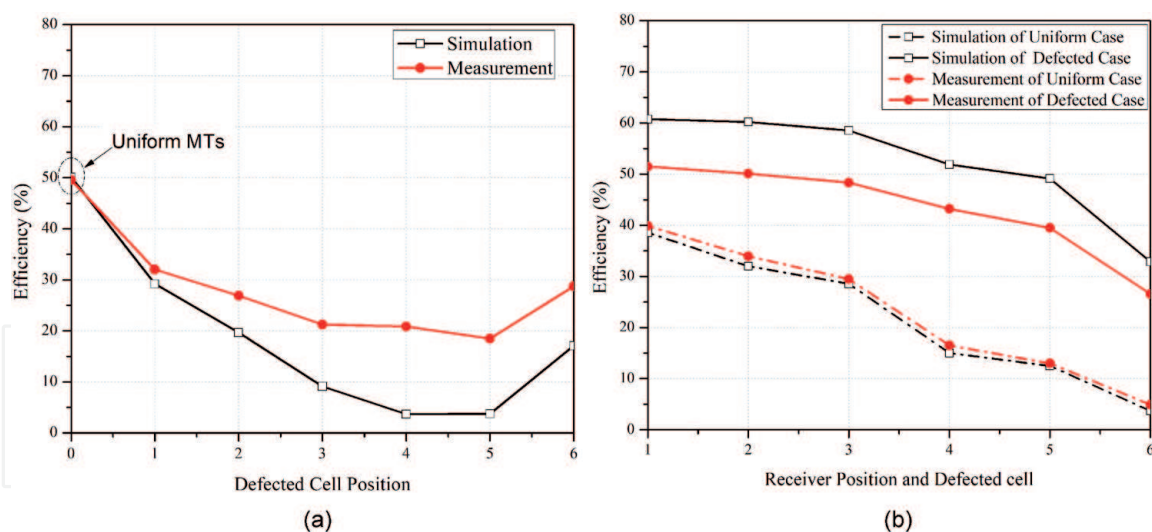


**Figure 9.**

*Measured and simulated results of the transfer efficiency with the uniform or defected metasurface (a) LTLR and (b) LTSR.*

MTSs. We obtained the measured transfer efficiency of LTSR case of 51.5%, 50.1%, 48.3%, 43.2%, 39.5% and 26.6% at the receiver positions of No. 1 to No. 6, respectively. Contrastingly, for the uniform MTS, the efficiency decreases obviously, when the receiving positions are moved far away from the center since the intensity of magnetic field at the edge is lower than at the center for the uniform MTS.

## 4. Conclusions

In this chapter, we propose the defected MTS for enhancing transferred efficiency and reducing the EMF. The MTS is based on a defected unit cell at the desired receiving position formed two-dimensional cavity. It can improve the localization of the magnetic field; thus, the strong confinement of the receiving location can be realized. Compared to previous defected MTSs especially in case of the small transmitter, using this proposed method, it is a simple way to create the cavity of two-dimension area because the single unit cell is only used and controlled in contrast of the series of an array of the defected unit cells via hopping or MIW route. The power transfer efficiency of the proposed defected MTS increases significantly from 1.9% (free space case) and 38% (uniform MTS) to 60% with the size ratio between transmitter and receiver is 4:1. Moreover, the confinement can reduce the leakage EMF around the surrounding system without additional shielding box. It can reduce EMF leakage about 10 to 15 dB at 13.56 MHz with the defected MTS. When the defected MTS is integrated in the WPT system, however, the size of the receivers is affected of the overall efficiency. If the size of the receiver is comparable compared with the unit cell size, it gets better efficiency than the larger receivers. Consequently, the defected MTS is not suitable for the case of the large transmitting and receiving coils due to splitting frequency effect. We hope that thought the proposed defected MTS operates in low frequency, the proposed structure can be easily scaled and tuned by adjusting the geometry of the coil and changing the capacitor value.

## Acknowledgements

This work was supported by the Thailand Research Fund under Grant RSA6280056.

## **Conflict of interest**

The authors declare no conflict of interest.

IntechOpen

## **Author details**

Sarawuth Chaimool<sup>1\*</sup>, Chawalit Rakluea<sup>2</sup>, Yan Zhao<sup>3</sup> and Prayoot Akkaraekthalin<sup>2</sup>

1 Electrical Engineering, Faculty of Engineering, Khon Kaen University,  
Khon Kaen, Thailand

2 Electrical and Computer Engineering, Faculty of Engineering, King Mongkut's  
University of Technology North Bangkok, Bangkok, Thailand

3 International School of Engineering, Faculty of Engineering, Chulalongkorn  
University, Bangkok, Thailand

\*Address all correspondence to: [sarachai@kku.ac.th](mailto:sarachai@kku.ac.th); [jaounarak@gmail.com](mailto:jaounarak@gmail.com)

## **IntechOpen**

© 2021 The Author(s). Licensee IntechOpen. This chapter is distributed under the terms of the Creative Commons Attribution License (<http://creativecommons.org/licenses/by/3.0>), which permits unrestricted use, distribution, and reproduction in any medium, provided the original work is properly cited. 

## References

- [1] iPhone12 [Internet]. 2020. Available from <https://support.apple.com/en-us/HT211829>
- [2] Qi standard [Internet]. 2020. Available from <https://www.wirelesspowerconsortium.com/qi/>
- [3] Mi C, Buja G, Choi S, Rim C: Modern advances in wireless power transfer systems for roadway powered electric vehicles. *IEEE Trans. Ind. Electron.* 2016;10:6533-6545. DOI: 10.1109/TIE.2016.2574993.
- [4] Patil D, McDonough M, Miller J, Fahimi B, Balsara P: Wireless power transfer for vehicular applications: overview and challenges. *IEEE Trans. Transp. Elect.* 2018; 4: 3-37. DOI: 10.1109/TTE.2017.2780627.
- [5] Panchal C, Stegen S, Lu J: Review of static and dynamic wireless electric vehicle charging system: *Int. J. Eng. Sci. Tech.* 2018; 21:922-937. DOI: 10.1016/j.jestch.2018.06.015
- [6] Garnica J, Chinga R, Lin J: Wireless power transmission: from far field to near field. *IEEE Proc.* 2013;101: 1321-1331. DOI: 10.1109/JPROC.2013.2251411.
- [7] Corrêa D, Resende U, Bicalho F: Experiments with a compact wireless power transfer system using strongly coupled magnetic resonance and metamaterials. *IEEE Trans. Magn.* 2019;55: 8401904. DOI: 10.1109/TMAG.2019.2913767
- [8] Huang R, Zhang B: Frequency, impedance characteristics and hf converters of two-coil and four-coil wireless power transfer. *IEEE J. Emerg. Sel. Pow. Electron.* 2015; 3:177-183. DOI:10.1109/JESTPE.2014.2315997.
- [9] Cheon S, Kim Y, Kang S, Lee M, Lee J, Zyung T: Circuit-model-based analysis of a wireless energy-transfer system via coupled magnetic resonances. *IEEE Trans. Ind. Electron.* 2010;58: 2906-2914. DOI: 10.1109/TIE.2010.2072893.
- [10] Hui S. Y. R, Zhong W, Lee C. K.: A critical review of recent progress in mid-range wireless power transfer. 2013;29: 4500-4511. DOI: 10.1109/TPEL.2013.2249670.
- [11] ICNIRP. Guidelines for limiting exposure to electromagnetic fields (100 kHz to 300 GHz). *Health Phys* 118(00):000-000; 2020. Pre-print. DOI: 10.1097/HP.0000000000001210.
- [12] Song C, Kim H, Jung D. H, Kim J, Kong S, Kim J, Ahn S, Kim J, Kim J: Low EMF and EMI design of a tightly coupled handheld resonant magnetic field (HH-RMF) charger for automotive battery charging. *IEEE Trans. Electromag. Compat.* 2016; 58: 1194-1206. DOI: 10.1109/TEMC.2016.2557842.
- [13] Park H, Kwon J, Kwak S, Ahn S: Effect of airgap between a ferrite plate and metal strips on magnetic shielding. *IEEE Trans. Magn.* 2015; 51: 9401504. DOI: 10.1109/TMAG.2015.2432102.
- [14] Li J, Yin F, Wang L, Wang L: Research on the transmission efficiency of different shielding structures of wireless power transfer system for electric vehicles. *CSEE J. Pow. Ener. Sys.* 2020; DOI: 10.17775/CSEEJPES.2019.00500.
- [15] Ranaweera A, Moscoso C, Lee J: Anisotropic metamaterial for efficiency enhancement of mid-range wireless power transfer under coil misalignment. *J. Phys. D: Appl. Phys.* 2015; 48:455104(8pp). DOI:10.1088/0022-3727/48/45/455104.
- [16] Younesiraad H, Bemani M: Analysis of coupling between magnetic dipoles

enhanced by metasurfaces for wireless power transfer efficiency improvement. *Sci. Reports*. 2018; 8:14865. DOI: 10.1038/s41598-018-33174-8.

[17] LI L, Liu H, Zhang H, Xue W: Efficient wireless power transfer system integrating with metasurface for biological applications. *IEEE Trans. Indus. Electron*. 2018; 4:3230-3239. DOI: 10.1109/TIE.2017.2756580.

[18] Rakluea C, Chaimool S, Zhao Y, Akkaraekthalin P: Compact non-uniform metasurface for efficiency enhancement of planar wireless power transfer. In: *Proceedings of the 2019 International Electrical Engineering Congress (iEECON2019)*, 6-8 March 2019, Cha-am, Thailand. New York: IEEE; 2019. p.1-4

[19] Lee W, Yoon Y: Wireless power transfer systems using metamaterials: A review. *IEEE Access*. 2020; 8: 147930-147947. DOI: 10.1109/ACCESS.2020.3015176.

[20] Bui H, Pham T, Ngo V, Lee J: Investigate of various cavity configurations for metamaterial-enhanced field-localizing wireless power transfer. *J. Appl. Phys*. 2017; 122:093102-093110. DOI: 10.1063/1.5001130.

[21] Lu C, Huang X, Rong C, Hu Z, Chen J, Tao X, Wang S, Wei B, Liu M: Shielding the magnetic field of wireless power transfer system using zero-permeability metamaterial. *J. Eng*. 2019; 16:1812-1815. DOI: 10.1049/joe.2018.8678.

[22] Cho Y, Lee S, Kim D, Kim H, Song C, Kong S, Park J, Seo C, Kim J: Thin hybrid metamaterial slab with negative and zero permeability for high efficiency and low electromagnetic field in wireless power transfer systems. *IEEE Trans. Electromagn. Compat*. 2017; DOI: 10.1109/TEMC.2017.2751595.

[23] Bui H, Kim J, Lee J: Design of tunable metasurface using deep neural networks for field localized wireless power transfer. *IEEE Access*. 2020; 8:194868-194878. DOI: 10.1109/Access.2020.3033527.

[24] Bui H, Pham T, Kim J, Lee J: Field-focused reconfigurable magnetic metamaterial for wireless power transfer and propulsion of an untethered microrobot. *J. Magn. Mater*. 2020; 494:165778. DOI: 10.1016/j.jmmm.2019.165778.

[25] Pham T, Ranaweera A, Lam V, Lee J: Experiments on localized wireless power transmission using a magneto-inductive wave two-dimensional metamaterial cavity. *Appl. Phys. Exp*. 2016; 9:044101. DOI: 10.7567/APEX.9.044101.

[26] Shamonica E, Kalinin V, Solymar L: Magnetoinductive waves in one, two, and three dimensions. *J. Appl. Phys*. 2002; 92:6252-6261. DOI:10.1063/1.1510945.

[27] Sandoval F, Delgado S, Moazenzadeh A, Wallrabe U: A 2-D magnetoinductive wave device for freer wireless power transfer. *IEEE Trans. Power Electron*. 2019; 34: 10433-10445. DOI: 10.1109/TPEL.2019.2904875.

[28] Stevens C: Magnetoinductive waves and wireless power transfer. *IEEE Trans. Power Electron*. 2014; 30: 6182-6190. DOI: 10.1109/TPEL.2014.2369811.

[29] Campione S, Mesa F, Capolino F: Magnetoinductive waves and complex modes in two-dimensional periodic arrays of split ring resonators. *IEEE Trans. Antennas Propag*. 2013; 61: 3554-3563. DOI: 10.1109/TAP.2013.2258395.

[30] Pham T, Ranaweera A, Ngo D, Lee J: Analysis and experiments on Fano interference using a 2D metamaterial cavity for field localized wireless power transfer. *J. Phys. D: Appl*.

Phys. 2017; 50:305102(10pp). Doi:  
10.1088/1361-6463/aa7988.

[31] Chaimool S, Rakluea C, Akkaraekthalin P, Zhao Y: Effect of losses in printed rectangular coils for compact wireless power transfer systems. Prog. Electromag. Research C. 2019; 97:177-188. DOI:10.2528/PIERC19092601.

[32] CST Microwave Studio, Computer Simulation Technology, Framing-ham, MA, 2015.

[33] Ranaweera A, Pham T, Bui N, Ngo V, Lee J: An active metasurface for field-localizing wireless power transfer using dynamically reconfigurable cavities. Sci. Rep. 2019; 9:11735. DOI: 10.1038/s41598-019-48253-7.

[34] Lyu Y, Meng F, Yang G, Che B, Wu Q, Sun L, Ermi D, Li J: A method of using nonidentical resonant coils for frequency splitting elimination in wireless power transfer. IEEE Trans. Power Electron. 2015; 30:6097-6107. DOI: 10.1109/TPEL.2014.2387835.

[35] Lv B, Li R, Fu J, Wu Q, Zhang K, Chen W, Wang Z, Ma R: Analysis and modeling of Fano resonances using equivalent circuit elements. Sci. Rep. 2016; 6:31884. DOI: 10.1038/srep31884.